A Serine → Cysteine Ligand Mutation in the High Potential Iron−Sulfur Protein from *Chromatium vinosum* Provides Insight into the Electronic Structure of the [4Fe−4S] Cluster

Elena Babini,[†,‡] Ivano Bertini,*[,§,||] Marco Borsari,[⊥] Francesco Capozzi,[†] Alexander Dikiy,[§] Lindsay D. Eltis,[‡,||] and Claudio Luchinat[†,||]

Contribution from the Institute of Agricultural Chemistry, University of Bologna, Viale Berti Pichat, 10 40127 Bologna, Italy, Department of Biochemistry, Université Laval, Québec City, Québec G1K 7P4, Canada, Department of Chemistry, University of Florence, Via Gino Capponi, 7, 50121 Florence, Italy, and Department of Chemistry, University of Modena, Via Campi 183, 41100 Modena, Italy

Received August 4, 1995[⊗]

Abstract: We have succeeded in preparing a mutant of the High Potential Iron−Sulfur Protein (HiPIP) from *Chromatium vinosum* in which a cysteine ligand has been replaced by a serine (C77S). Proton chemical shift data and nuclear Overhauser effects indicate that structural perturbations induced by the C77S mutation are minimal in both the oxidized and reduced forms of the HiPIP. The reduction potential of C77S is 25 mV lower than that of the wild-type HiPIP (WT) (0.2 M ionic strength, pH 4.5−9.0, 25 °C). Assignment of the hyperfine shifted signals in the ^{1}H NMR spectrum of oxidized C77S revealed that the temperature dependences of the signals associated with cluster-ligating residues 46 and 77 are Curie and anti-Curie type, respectively, and are thus the reverse of those in WT. Taken together, these observations indicate that the iron bound to Ser-77 is less reducible than the corresponding iron in WT. The results are consistent with a previous model of the electronic structure of oxidized HiPIP clusters, confirming the presence of an equilibrium between two species of differing valence distributions. The current results permit the extension of this model to predict the relative reduction potentials of the individual iron ions in the oxidized HiPIPs up to now investigated.

Introduction

The investigation of the electronic structure of $[Fe_4S_4]^{n+}$ (n = 1, 2, 3) clusters has recently progressed significantly, but the underlying theoretical model is still the subject of intense debate.[1−11] The most studied system is the $[Fe_4S_4]^{3+}$ of HiPIPs, a class of proteins implicated in photosynthetic electron transfer in purple non-sulfur bacteria.[12] The $[Fe_4S_4]^{3+}$ cluster formally contains three Fe^{3+} and one Fe^{2+}. Mössbauer data at 4.2 K demonstrate the presence of two distinct pairs of iron ions. One pair of ions has an isomer shift typical of iron in the intermediate oxidation state $Fe^{2.5+}$, whereas the other pair has an isomer shift typical of Fe^{3+}.[13−15] Magnetic Mössbauer also provides the hyperfine coupling energy with ^{57}Fe. For the *C. vinosum* HiPIP, the hyperfine coupling constant A/h has been estimated to be −32.0 and 20.2 MHz for the mixed valence and ferric pairs, respectively.[14,16] In contrast, the A/h values for isolated Fe^{2+} and Fe^{3+} in $Fe(SR)_4^{1-/2-}$ moieties are −22 and −20 MHz, respectively.[17,18] The reversal in sign of the hyperfine coupling constant of the ferric pair in the $[Fe_4S_4]^{3+}$ has been ascribed to the effect of antiferromagnetic coupling between the ferric and the mixed valence pairs, the ferric pair having a smaller subspin than the mixed valence pair.[14,15] The hyperfine couplings with the protons of the coordinated cysteines obtained at room temperature through NMR are consistent with this interpetation, although these data provide much more information than Mössbauer data due to their higher resolution.[19−26]

The NMR spectroscopy of paramagnetic compounds has now progressed to the point where the ligand protons may be readily sequence-specifically assigned.[27] The eight β-CH_2 protons of

* Address correspondence to this author at the University of Florence.
† University of Bologna.
‡ Université Laval.
§ University of Florence.
|| To whom reprint requests should be sent.
⊥ University of Modena.
⊗ Abstract published in *Advance ACS Abstracts,* December 1, 1995.

(1) Noodleman, L. *Inorg. Chem.* **1991**, *30*, 246−256.
(2) Noodleman, L. *Inorg. Chem.* **1991**, *30*, 256−264.
(3) Noodleman, L. *Inorg. Chem.* **1988**, *27*, 3677−3679.
(4) Noodleman, L.; Case, D. A. *Adv. Inorg. Chem.* **1992**, *38*, 424−470.
(5) Belinskii, M.; Bertini, I.; Galas, O.; Luchinat, C. *Z. Naturforsch.* **1995**, *50a*, 75−80.
(6) Belinskiy, M. I.; Bertini, I.; Galas, O.; Luchinat, C. *Inorg. Chim. Acta* **1995**, in press.
(7) Bertini, I.; Ciurli, S.; Luchinat, C. In *Structure and Bonding*; Springer−Verlag: Berlin, Heidelberg, 1995; Vol. 83, pp 1−54.
(8) Bominaar, E. L.; Borshch, S. A.; Girerd, J.-J. *J. Am. Chem. Soc.* **1994**, *116*, 5362−5372.
(9) Mouesca, J. M.; Rius, G. J.; Lamotte, B. *J. Am. Chem. Soc.* **1993**, *115*, 4714−4731.
(10) Mouesca, J. M.; Lamotte, B.; Rius, G. J. *Inorg. Biochem.* **1991**, *43*, 251.
(11) Jordanov, J.; Roth, E. K. H.; Fries, P. H.; Noodleman, L. *Inorg. Chem.* **1990**, *29*, 4288−4292.
(12) Hochkoeppler, A.; Ciurli, S.; Venturoli, G.; Zannoni, D. *FEBS Lett.* **1995**, *357*, 70−74.
(13) Moss, T. H.; Bearden, A. J.; Bartsch, R. G.; Cusanovich, M. A. *Biochemistry* **1968**, *7*, 1591−1596.
(14) Middleton, P.; Dickson, D. P. E.; Johnson, C. E.; Rush, J. D. *Eur. J. Biochem.* **1980**, *104*, 289−296.
(15) Bertini, I.; Campos, A. P.; Luchinat, C.; Teixeira, M. *J. Inorg. Biochem.* **1993**, *52*, 227−234.
(16) Dickson, D. P. E.; Johnson, C. E.; Cammack, R.; Evans, M. C. W.; Hall, D. O.; Rao, K. K. *Biochem. J.* **1974**, *139*, 105.
(17) Schulz, C.; Debrunner, P. G. *J. Phys. (Paris)* **1976**, *37*, C6-153.
(18) LeGall, J.; Prickril, B. C.; Moura, I.; Xavier, A. V.; Moura, J. J. G.; Huynh, B. H. *Biochemistry* **1988**, *27*, 1636−1642.
(19) Bertini, I.; Capozzi, F.; Luchinat, C.; Piccioli, M.; Vicens Oliver, M. *Inorg. Chim. Acta* **1992**, *198*−*200*, 483−491.
(20) Banci, L.; Bertini, I.; Ferretti, S.; Luchinat, C.; Piccioli, M. *J. Mol. Struct.* **1993**, *292*, 207−220.
(21) Bertini, I.; Capozzi, F.; Ciurli, S.; Luchinat, C.; Messori, L.; Piccioli, M. *J. Am. Chem. Soc.* **1992**, *114*, 3332−3340.

0002-7863/96/1518-0075$12.00/0

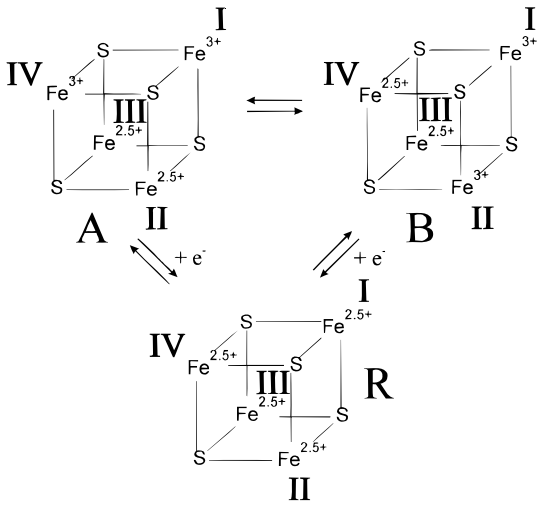

Figure 1. Cubane [4Fe−4S] clusters in iron−sulfur proteins. Cysteine ligands are omitted for clarity; however, the irons have been numbered after the order of the occurrence of their respective cysteine ligand in the amino acid sequence. The scheme shows equilibria among two different oxidized and one reduced species in HiPIPs. Species A and B differ in the position of the mixed valence pair (on irons II and III in species A and on irons III and IV in species B).

the four coordinated cysteines in a series of $[Fe_4S_4]^{3+}$-containing proteins appear strongly inequivalent. This inequivalence can be rationalized in terms of three factors: the intrinsic asymmetry of the protein; the dependence of the hyperfine coupling on the Fe−S−C−H dihedral angle; and the dependence of the hyperfine coupling on the Fe−Fe coupling scheme. Of these, the second two factors exert the greatest influence and are essentially independent of each other. The dependence of the hyperfine coupling on the dihedral angle renders the individual protons of each β-CH_2 pair inequivalent,[28] while the Fe−Fe coupling scheme differentiates the protons of each β-CH_2 pair from the others.[7]

Analysis of the hyperfine proton shifts in a series of HiPIPs in terms of the Fe−Fe coupling scheme has allowed some of us to propose the existence of an equilibrium between two species which would be fast on the NMR time scale.[24] These two species differ in the localization of the mixed valence pair (and consequently of the ferric pair) within the $[Fe_4S_4]^{3+}$ cluster as defined by the protein environment (see species A and B in Figure 1). Significantly, an equilibrium between just two isomers, as opposed to six possible isomers, is sufficient to explain the experimental data. The position of the equilibrium, *i.e*. the percentage of A and B species, varies from protein to protein. The $[Fe_4S_4]^{3+}$ cluster may be viewed as a hypothetical $[Fe_4S_4]^{4+}$ (with four Fe^{3+}) to which an electron is added. This electron localizes to the pair of iron ions possessing the higher reduction potential in the hypothetical $[Fe_4S_4]^{4+}$ cluster. In the proposed equilibrium between two forms, one iron is the most reducible (*i.e*. it is always $Fe^{2.5+}$) and one the least reducible (*i.e*. it is always Fe^{3+}) while the other two irons are $Fe^{2.5+}$ in one of the two species and Fe^{3+} in the other, and *vice versa*. The position of the equilibrium must be related to the electrostatic potential of each iron and to the electrostatic potential generated by the protein. Ultimately, the position of the equilibrium depends on the same electrostatic factors which determine the reduction potential of the whole protein. The ^{1}H NMR studies have been used to monitor the position of the equilibrium in solution at room temperature.

The current study is aimed at elucidating the relationship between the electronic structure in the $[Fe_4S_4]^{3+}$ and its reduction potential. Point mutations in recombinant *Ectothiorhodospira halophila* iso-I and *C. vinosum* HiPIPs that do not involve the cysteine ligands alter the reduction potential of the cluster less than 30 mV and no significant change in the equilibrium within the oxidized cluster is observed.[29,30] Attempts to perturb the electronic structure of the cluster by substituting the cluster-ligating residues led to the identification of a stable variant *C. vinosum* HiPIP in which Cys-77 had been replaced by serine. We report here the NMR and electrochemical characterization of this C77S variant. The insight that this characterization provides into the factors influencing the reducibility of the individual irons of the cluster is discussed.

Materials and Methods

Overexpression of a synthetic gene encoding *C. vinosum* HiPIP as a fusion protein was accomplished essentially as described for the gene encoding *E. halophila* iso-I HiPIP.[31] The C77S variant was obtained by oligonucleotide-directed mutagenesis as described elsewhere.[30,32−34] Recombinant *C. vinosum* HiPIP (rcWT) and C77S were purified to apparent homogeneity as described for *E. halophila* iso-I HiPIP[29] with slight modifications. The additional *N*-terminal amino acid (alanine 0) of rcWT does not appreciably alter the spectroscopic or electrochemical properties of the HiPIP.

Midpoint reduction potential values were determined by both square-wave voltammetry (SWV), using a frequency of 10 Hz and a pulse amplitude of 40 mV, and cyclic voltammetry (CV), at a scan rate 0.01−0.1 V/s. Electrochemical measurements were performed using a freshly polished pyrolytic graphite disc (edge plane) as the working electrode. The protein solution contained 2 mM neomycin and 0.15 M sodium chloride. A reversible, diffusion-controlled electrochemical process was observed. All the potentials were standardized to the normal hydrogen electrode (NHE). Other experimental details are the same as previously reported.[35]

^{1}H NMR spectra were recorded with an AMX 600 Bruker spectrometer operating at 600.14 MHz Larmor frequency. The spectra were calibrated assigning a shift of 4.81 ppm, with respect to DSS, to the residual HOD signal at 298 K. 1D NOE difference spectra were accumulated using described methodologies.[36,37]

Results

C77S is quite stable in both oxidation states over a pH range of 4.5−9.5. Below pH 4.5, the cluster decomposed without

(22) Banci, L.; Bertini, I.; Capozzi, F.; Carloni, P.; Ciurli, S.; Luchinat, C.; Piccioli, M. *J. Am. Chem. Soc*. **1993**, *115*, 3431−3440.
(23) Bertini, I.; Capozzi, F.; Luchinat, C.; Piccioli, M. *Eur. J. Biochem*. **1993**, *212*, 69−78.
(24) Banci, L.; Bertini, I.; Ciurli, S.; Ferretti, S.; Luchinat, C.; Piccioli, M. *Biochemistry* **1993**, *32*, 9387−9397.
(25) Bertini, I.; Gaudemer, A.; Luchinat, C.; Piccioli, M. *Biochemistry* **1993**, *32*, 12887−12893.
(26) Bertini, I.; Capozzi, F.; Eltis, L. D.; Felli, I. C.; Luchinat, C.; Piccioli, M. *Inorg. Chem*. **1995**, *34*, 2516−2523.
(27) Bertini, I.; Turano, P.; Vila, A. J. *Chem. Rev*. **1993**, *93*, 2833−2932.
(28) Bertini, I.; Capozzi, F.; Luchinat, C.; Piccioli, M.; Vila, A. J. *J. Am. Chem. Soc*. **1994**, *116*, 651−660.
(29) Iwagami, S. G.; Creagh, A. L.; Haynes, C. A.; Borsari, M.; Felli, I. C.; Piccioli, M.; Eltis, L. D. *Protein Sci*. **1995**, in press.
(30) Unpublished results from our laboratories.
(31) Eltis, L. D.; Iwagami, S. G.; Smith, M. *Protein Eng*. **1994**, *7*, 1145−1150.
(32) Ausubel, F. M.; Brent, R.; Kingston, R. E.; Moore, D. D.; Seidman, J. G.; Smith, J. A.; Struhl, K. *Current Protocols in Molecular Biology*; Greene Publishing Associates: New York, 1991.
(33) Kunkel, T. A.; Roberts, J. D.; Zakour, R. A. *Methods Enzymol*. **1987**, *154*, 267−382.
(34) Zoller, M. J.; Smith, M. *Methods Enzymol*. **1987**, *154*, 329−350.
(35) Luchinat, C.; Capozzi, F.; Borsari, M.; Battistuzzi, G.; Sola, M. *Biochem. Biophys. Res. Commun*. **1994**, *203*, 436−442.
(36) Dugad, L. B.; La Mar, G. N.; Banci, L.; Bertini, I. *Biochemistry* **1990**, *29*, 2263−2271.
(37) Banci, L.; Bertini, I.; Luchinat, C.; Piccioli, M.; Scozzafava, A.; Turano, P. *Inorg. Chem*. **1989**, *28*, 4650−4656.

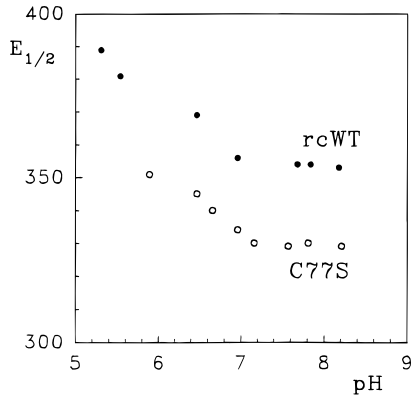

Figure 2. pH dependencies of the reduction potentials of the C77S and rcWT proteins. Experimental conditions are described in Experimental Section.

the detection of a $[Fe_3S_4]$ cluster, as followed by electronic absorption and circular dichroic spectroscopies. The midpoint reduction potential of C77S was determined to be 330 mV by cyclic voltammetry (150 mM sodium chloride, pH 7.0, 25 °C), while that of rcWT was determined to be 355 mV under similar conditions. This difference of 25 mV between the reduction potentials of C77S and rcWT was observed between pH 5.5 and 8.5 (Figure 2).

The ^{1}H NMR Spectra of the Oxidized Species. The spectrum of the oxidized C77S mutant is reported in Figure 3A together with that of WT. Both proteins show nine hyperfine shifted signals which arise from eight β-CH_2 and/or α-CH protons of the four coordinated ligands. The sequence-specific and stereospecific assignment of the variant was performed with a procedure similar to that used for the WT protein. Saturation of the hyperfine shifted signals (Figure 4) yields NOEs with signals in the diamagnetic region. The number and chemical shifts of these latter signals in C77S are very similar to those previously observed in WT.[21] This constitutes strong evidence that the residues in the immediate vicinity of the cluster, including Leu-17, Tyr-19, Phe-66, Leu-71, Val-73, Ala-78, and Trp-80, have essentially the same structure as in the WT.

Saturation of A yields NOE with C and with signals at 6.98, 6.57, and 1.89 ppm which are ascribed to NH, Hδ, and Hβ1 of Phe-66. Signal A is thus assigned to Hβ2 of Cys-63 and, consequently, signal C to Hβ1. Saturation of signals I and H yields NOEs to each other and with signals at 3.70 and 1.10 ppm, corresponding to Hα of Val-73 and δ-CH_3 of Ile-71, respectively. Comparison of the relative NOE intensities together with the observation of NOE between signal H and a signal at 10.09 ppm corresponding to NH of Cys-43 permits the assignment of signal H to Hβ1 of Cys-43 and of signal I to Hβ2. Saturation of signals B, D, and E yields NOEs to each other and to a signal at 5.19 ppm belonging to Hα of Tyr-19,[21] unambiguously identifying these signals as arising from the aliphatic protons of Ser-77. Saturation of B gives NOE to D and intense NOEs with NH of Ala-78 and the Hβ's of Leu-17, as in WT.[21] Signal B is thus assigned to the Hβ1 of Ser-77. Accordingly, signal D, corresponding to Hβ2 of Ser-77, shows a smaller NOE than B with NH of Ala-78, but gives an intense NOE with Hδ of Tyr-19 (6.76 ppm), as expected.[38] The assignment of signal E to Hα of Ser-77 by default is confirmed by its dipolar connectivities with NH of Ala-78 and Hϵ of Trp-76. Signals F and G must arise from the β-CH_2 protons of Cys-46. The pattern of NOE connectivities observed by saturating signal F (NHϵ of Trp-80, NH of Cys-46, Hα of Cys-43 and Cys-46) assigns signal F to Hβ1 of Cys-46. Signal G is thus assigned to Hβ2 of Cys-46. The sequence-specific and stereospecific assignment of the oxidized species together with WT is summarized in Table 1.

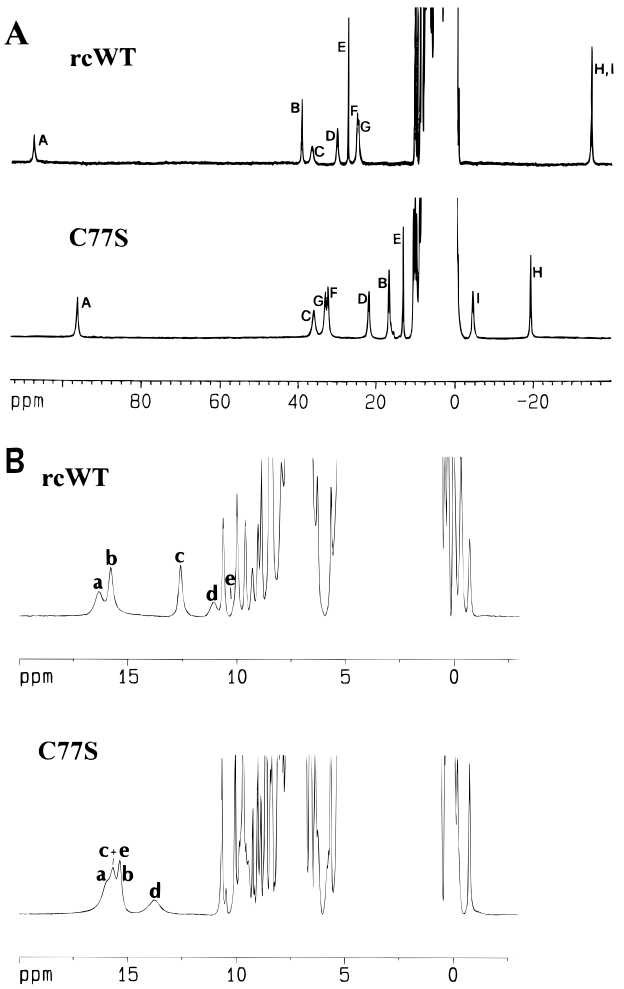

Figure 3. 600-MHz ^{1}H NMR spectra of oxidized (A) at 298 K and reduced (B) at 290 K rcWT and C77S *C. vinosum* HiPIP at pH 7.0, 50 mM Pi.

The temperature dependence of the hyperfine shifted signals is shown in Figure 5, together with that of rcWT for comparison purposes. As summarized in Table 1, the temperature dependences of the hyperfine shifts of protons of Cys-63 and Cys-43 are the same in the two proteins. On the other hand, the hyperfine shifted signals of residues 77 and 46 have reversed their behavior from one protein to the other. The significance of these temperature dependences with respect to the equilibrium model of Figure 1 and the reduction potential of the individual irons is discussed below.

The ^{1}H NMR Spectra of the Reduced Form. The ^{1}H NMR spectra of reduced C77S and rcWT are shown in Figure 3B. All the hyperfine shifted signals in these two HiPIPs show the anti-Curie temperature dependence typical of $[Fe_4S_4]^{2+}$ cluster ligands.[7] Analogously to the rcWT, the iron ions of C77S are at the oxidation state +2.5 and the ground state is $S = 0$.[7] Population of the exited levels provides some paramagnetism. The assignment of the β-CH_2 ligand protons was obtained by 1D NOE difference spectra, saturating hyperfine shifted signals, and is reported in Table 1. 1D NOE difference spectra have allowed us to detect the β-CH_2 signals located in the diamagnetic region. The details of the assignment procedure are essentially the same as those reported for the oxidized species and are thus

(38) Carter, C. W. J.; Kraut, J.; Freer, S. T.; Xuong, N.-H.; Alden, R. A.; Bartsch, R. G. *J. Biol. Chem.* **1974**, *249*, 4212−4215.

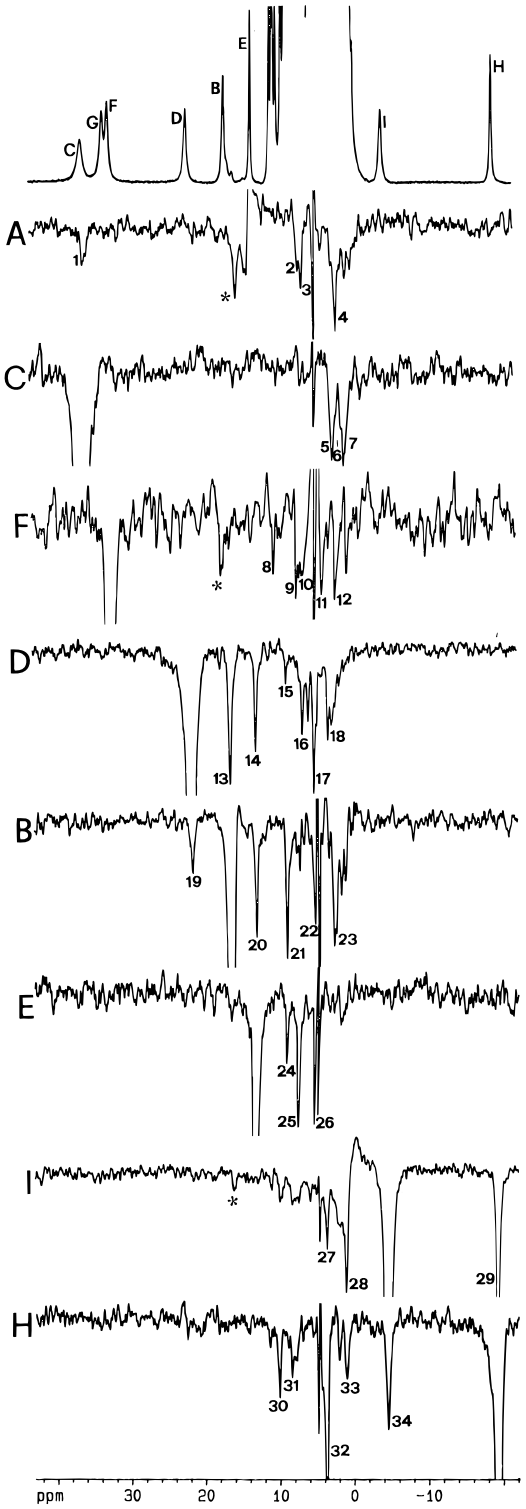

Figure 4. ^{1}H 600-MHz 290 K NMR spectra of the oxidized C77S from *Chromatium vinosum*: upper trace, reference spectrum; lower traces, NOE difference spectra. The latter are labeled according to which signal is saturated. The assignment of the detected NOEs is as follows: (1) Hβ_2 Cys-63, (2) NH Phe-66, (3) Hδ Phe-66, (4) Hβ Phe-66, (5) Hγ Ile-71, (6) Hβ Phe-66, (7) γ-CH$_3$ Ile-71, (8) NHϵ Trp-80, (9) NH Cys-46, (10) NH Asn-45, (11) Hα Cys-43, (12) Hα Cys-46, (13) Hβ_2 Ser-77, (14) Hα Ser-77, (15) NH Ala-78, (16) Hδ Tyr-19, (17) Hα Tyr-19, (18) Hβ Tyr-19, (19) Hβ_3 Ser-77, (20) Hα Ser-77, (21) NH Ala-78, (22) Hα Tyr-19, (23) Hβ Leu-17, (24) NH Ala-78, (25) Hϵ Trp-76, (26) Hα Tyr-19, (27) Hα Val-73, (28) δ-CH$_3$ Ile-71, (29) Hβ_2 Cys-43, (30) NH Cys-43, (31) NH Ala-44, (32) Hα Val-73, (33) δ-CH$_3$ Ile-71, (34) Hβ_3 Cys-43. Signals which are due to saturation transfer effects to the corresponding protons in the reduced form are marked by an asterisk.

omitted. Inspection of Table 1 reveals that the sequence-specific assignments in C77S correspond very closely to those in rcWT.

Discussion

The current results indicate that the structure of the C77S variant, particularly of the cluster environment, is very similar to that of WT: the cluster is intact and Ser-77 is ligated to one of the irons. This is true of both oxidized and reduced forms of C77S. This conclusion is based on the chemical shifts of the protons to which the hyperfine shifted signals of C77S show NOEs as well as the intensities of the NOEs between these signals and is being confirmed by the solution structure of the protein.[39] To a first approximation, it is thus possible to rationalize the differences between C77S and WT by considering the chemical consequences of replacing the sulfur of Cys-77 with oxygen. The decrease in the reduction potential of C77S is thus consistent with the larger electronegativity of oxygen with respect to sulfur, but is perhaps surprisingly modest given the severity of the substitution.

The substitution of Cys-77 with serine probably results in subtle structural changes that could manifest themselves by changes in the Fe−S−C−H dihedral angles, θ. As mentioned above, these angles differentiate the two protons within each β-CH$_2$ pair.[28] The chemical shift may also reflect bond strength as related to the charge on the iron. Thus, the substitution-induced changes of signals I and H may reflect rearrangement of Cys-43 in oxidized C77S through either the Fe−S or S−Cβ bonds. The dihedral angles involving this residue vary widely in the HiPIPs studied and are even sensitive to temperature.[21−24,26,40,41]

The substitution-induced changes in the signals of the Hβ protons of Cys-63 (A and C) are minor in relation to the large shifts and the extreme θ values. The same holds for signals of the Hβ protons of Cys-46 (F and G). Finally, the shifts of signals B, D, and E are not perturbed very much although they belong to the mutated residue. While the shifts of the β-CH$_2$ signals B and D are reversed, it is noted that the substitution of a sulfur with an oxygen is expected to alter the dependence of the shift on the dihedral angle. Interestingly, our analysis of C77S provides no insight into why residue 77 is the only ligand whose Hα proton is observed outside the diamagnetic region.

The most meaningful substitution-induced difference concerns the temperature dependences of the chemical shifts of the five hyperfine shifted signals of residues 77 and 46. Those of residue 77 exhibit anti-Curie behavior in C77S (*i.e.*, increase with increasing temperature) and Curie behavior in rcWT (*i.e.*, decrease with increasing temperature). Concomitantly, those of Cys-46 exhibit Curie behavior in C77S and anti-Curie[7] behavior in rcWT. All five of these signals are downfield.

As described in the introduction, the electronic structure of the [Fe$_4$S$_4$]$^{3+}$ cluster can be described as an equilibrium between two species each of them being formed by a mixed-valence pair and a ferric pair. The nuclei of the ligands of the ferric pair experience negative hyperfine coupling and upfield shifts, whereas the ligands of the mixed-valence pair experience positive hyperfine coupling and downfield shifts. When an equilibrium between two species like that depicted in the upper part of Figure 1 exists that is fast on the NMR time scale, there is one iron which always is Fe^{3+} (iron I in Figure 1) and another which always is mixed valence (iron III in Figure 1). Their

(39) Bentrop, D.; Bertini, I.; Capozzi, F.; Dikiy, A.; Eltis, L.; Luchinat, C. Submitted for publication.

(40) Banci, L.; Bertini, I.; Dikiy, A.; Kastrau, D. H. W.; Luchinat, C.; Sompornpisut, P. *Biochemistry* **1995**, *34*, 206−219.

(41) Banci, L.; Bertini, I.; Carloni, P.; Luchinat, C.; Orioli, P. L. *J. Am. Chem. Soc.* **1992**, *114*, 10683−10689.

Table 1. Summary of the ^{1}H NMR Assignment of the Ligand Proton Signals of the rcWT[42] and C77S Variant of the Reduced and Oxidized HiPIP from *C. vinosum*

	reduced[a]				oxidized[b]		
			chemical shift, ppm			chemical shift, ppm[d]	
	proton	signal	rcWT	C77S	signal	rcWT	C77S
Cys-43	Hβ1	y[c]	7.19	7.63	H	−34.83 [pC]	−19.27 [pC]
	Hβ2	a	16.20	15.91	I	−34.83 [pC]	−4.48 [pC]
Cys-46	Hβ1	e	10.05	15.66	F	24.87 [aC]	32.52 [C]
	Hβ2	d	11.01	13.75	G	24.55 [aC]	33.24 [C]
Cys-63	Hβ1	z[c]	5.27	5.76	C	36.52 [C]	36.02 [C]
	Hβ2	b	15.78	15.35	A	107.68 [C]	96.41 [C]
	Hα		3.70	3.69			
Cys/Ser-77	Hβ1	c	12.60	15.66	B	39.13 [C]	16.33 [aC]
	Hβ2	w[c]	7.79	7.42	D	29.99 [C]	21.56 [aC]
	Hα	v[c]	8.23	8.10	E	27.21 [C]	13.03 [aC]

[a] At 290 K. [b] At 298 K. [c] Signals detected through 1D NOE. [d] Temperature dependence (C = Curie, aC = antiCurie, pC = pseudoCurie) in square brackets.

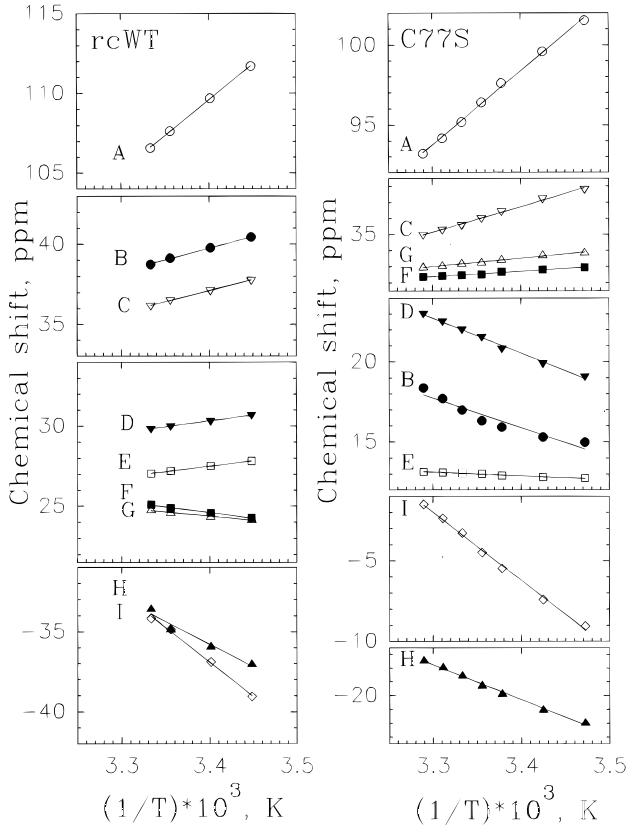

Figure 5. Experimental temperature dependencies of the hyperfine shifted signals of the oxidized rcWT and C77S *C. vinosum* HiPIP.

proton shifts are upfield and downfield, respectively. The ligand protons of the other two irons (irons II and IV in Figure 1), which change the oxidation state depending on the equilibrium, have intermediate shifts. However, one iron will be ferric more than 50%, and the other will be mixed valence by the same percentage. The ligand protons of these two iron ions will experience weighted average shifts intermediate between those of iron III (downfield) and iron I (upfield). Therefore, the protons belonging to the domain of the iron more than 50% mixed valence will be more downfield than those of the iron more than 50% ferric. The temperature dependencies will also be weighted averages: by lowering the temperature, the signals of the iron which is more than 50% mixed valence will tend to move downfield, following the same temperature dependence (Curie type) as iron III; conversely, the iron which is more than 50% ferric will tend to move upfield (anti-Curie), following the same temperature dependence of iron I (that had been termed pseudo-Curie,[7] as the signals of the latter domain are already upfield). Taking the average value of the two hyperfine shifts within each β-CH_2 pair of residues 46 and 77 (that corresponds to quenching the influence of the dihedral angle) permits the estimation of the extent of $Fe^{2.5+}$ and Fe^{3+} character of the corresponding irons.[26] This is achieved by taking the average value of the two β-CH_2 proton shifts of Cys-43 as the limiting value for 100% Fe^{3+} and the average value of the two Cys-63 β-CH_2 proton shifts as the limiting value for 100% $Fe^{2.5+}$.[26] The obtained estimate of the extent of $Fe^{2.5+}$ and Fe^{3+} character of each iron can in turn be used to estimate the equilibrium constant of the process shown in Figure 1. Though quite rough, such an estimate is qualitatively supported by the temperature dependence of the shifts. When the hyperfine shift is far downfield and exhibits a Curie-type temperature dependence, the degree of $Fe^{2.5+}$ character of the corresponding iron is in the range 60−90%, and its value can be estimated within ±5% error. An essentially temperature independent behavior is expected for a 50%:50% species distribution, as the Curie and anti-Curie behavior of the two contributing species tends to compensate.[24] These considerations provide the means to establish the relative reduction potential of each iron.

Within this framework, it is clear that Cys-77 of rcWT is bound to an iron which is predominantly $Fe^{2.5+}$, while the equivalent iron in C77S, which is bound to Ser-77, is predominantly Fe^{3+}. This makes sense chemically as oxygen is expected to increase the charge of the iron. The substitution of Cys-77 with serine thus causes a decrease in both the reducibility of the iron bound to residue 77 and the reducibility of the entire cluster. Of particular note, the decreased mixed-valence character of this iron is accompanied by an increase in the mixed-valence character of the iron bound to Cys-46. Unfortunately, we cannot prove that oxygen is bound as an anion rather than as a neutral donor. We can only speculate that the presence of a proton would provide serious changes in the reduction potential and in the structure around the cluster. The solution structure shows an extraordinary similarity in the structures of WT and mutant species.[39,42]

From the present data we can estimate that the iron bound to residue 77 is about 60% ± 5% $Fe^{2.5+}$ character in rcWT, as opposed to 35% ± 5% in C77S. This estimate assumes that only two of six possible species are significantly present in solution. The presence in C77S of a barely detectable third species, with different localization of the mixed-valence pair, could in principle account for the relatively small upfield shifts of signals I and H.

(42) While this paper was being typeset, we obtained experimental evidence of serinate coordination through capillary electrophoresis experiments.[39]

Table 2. Summary of Thermodynamic Parameters Obtained by Combining Potentiometric Data with NMR Data[a]

	rcWT	C77S
$\Delta G_{(A\rightarrow B)}$, kJ mol^{-1}	−1.53	1.00
$E_{m(A\rightarrow R)}$, mV	361	324
$E_{m(B\rightarrow R)}$, mV	351	340

[a] The estimated errors of ±5 mV in ΔE_m values (see text) are a function of the errors in the equilibrium percentages estimated from NMR.

Insight into the Reduction Potential of the Individual Ions. Simple thermodynamic considerations provide semiquantitative information on the reduction potentials of the individual iron atoms. In the thermodynamic cycle for both rcWT and C77S (Figure 1), reduction of species A or B, which are themselves in equilibrium, produces the same species, R. NMR has confirmed that in the reduced cluster of all HiPIPs including C77S, the spins are distributed essentially uniformly over the four irons.[23,43] The thermodynamic cycle of Figure 1 is defined by the following equations:

$$\Delta G_{(A\rightarrow B)} = \Delta G_{(A\rightarrow R)} + \Delta G_{(R\rightarrow B)} = \Delta G_{(A\rightarrow R)} - \Delta G_{(B\rightarrow R)} \quad (1)$$

In turn, $\Delta G_{(A\rightarrow B)}$ can be expressed in terms of the molar fractions of the A and B species obtained from NMR:

$$\Delta G_{(A\rightarrow B)} = -RT \ln K_{(A\rightarrow B)} = -RT \ln (f_B/f_A) \quad (2)$$

Finally, from the experimentally determined reduction potential of the cluster, E_m, we can write:

$$f_A \Delta G_{(A\rightarrow R)} + f_B \Delta G_{(B\rightarrow R)} = -FE_m \quad (3)$$

where F is Faraday's constant. From these three equations, $\Delta G_{(AB)}$, $\Delta G_{(AR)}$, and $\Delta G_{(BR)}$ can be estimated. The error in these estimates derives from the error in the molar fractions of the A and B species obtained from NMR measurements (see above). The reduction potentials of the A → R and B → R processes are given by:

$$-E_{m(A\rightarrow R)} = \frac{1}{F}\Delta G_{(A\rightarrow R)}; \quad -E_{m(B\rightarrow R)} = \frac{1}{F}\Delta G_{(B\rightarrow R)} \quad (4)$$

These potentials are reported in Table 2 for both rcWT and C77S. The replacement of cysteine 77 by serine lowers the reduction potential of species A by 37 ± 5 mV, and that of species B by 11 ± 5 mV. This result confirms that as a consequence of oxygen coordination to iron IV, the reduction of species A, which involves the reduction of the pair of irons I and IV, is appreciably more disfavored with respect to that of species B, which involves reduction of the pair of irons I and II.

Considering the hypothetical $[Fe_4S_4]^{4+}$ cluster containing four ferric irons, the relative magnitudes of the reduction potentials of each iron in the cluster are:

$$\text{iron III} \gg \text{iron IV} \approx \text{iron II} \gg \text{iron I}$$

In particular, the E_m of iron IV is slightly higher than that of iron II in HiPIPs from *R. gelatinosus*, *R. fermentans*, *C. vinosum*, and *E. vacuolata* Iso I and Iso II, based on the spin equilibrium in the respective oxidized proteins.[26] Similarly, the E_m of iron IV is slightly lower than that of iron II in HiPIPs from *R globiformis* and *E. halophila* Iso I and Iso II, as well as in the present C77S variant of *C. vinosum* HiPIP.

In conclusion, we note that in no $[Fe_4S_4]^{2+}$ species, regardless of whether it occurs in a reduced HiPIP (including the present variant) or oxidized ferredoxin, has there been any evidence for the existence of an iron in the 3+ state: all four irons have an equivalent oxidation state of 2.5+. This observation can be interpreted in terms of electron delocalization over two mixed valence pairs, which presumably further stabilizes the system.[8] The reduction of the HiPIP $[Fe_4S_4]^{3+}$ cluster may thus be viewed principally as reduction of the one iron ion (iron I) which is ferric or predominantly ferric. It may then be predicted that *increasing* the individual reduction potential of iron I should increase the overall E_m value of the cluster to a greater degree than equivalent changes in the individual E_m values of the other irons. At its limit, this reasoning would indicate that large increases in the reduction potential of iron I would be the most effective way of converting a HiPIP to a ferredoxin. Indeed, ferredoxins have a reduction potential so high for the $[Fe_4S_4]^{3+}$ state that the cluster is stable only at the $[Fe_4S_4]^{2+}$ state, and can be further reduced to $[Fe_4S_4]^{+}$, although with a relatively large negative reduction potential. Variants designed to test this hypothesis are currently being created. The present insight into the microscopic reduction potentials of component metal ions in a series of iron−sulfur proteins may thus lead to a deeper understanding of the factors affecting the reduction potentials in metalloproteins, and why nature selects polymetallic systems for particular redox tasks.

Acknowledgment. This work has been partially financed by Progetto Finalizzato Biotechnologie, Comitato Biotecnologie e Biologia Moleculare, and Comitato Scienze Agrarie of CNR, Italy. Some of the described work was performed in the laboratory of Dr. Michael Smith whose enthusiasm and support, particularly through the Protein Engineering Network Centres of Excellence, are gratefully acknowledged. Dr. John Hobbs, Debra M. Neufeld, Tracy J. Farr, and Tracy B. Evans at the University of British Columbia of the NAPS unit are thanked for synthesis of oligonucleotides and for running the sequencing gels. A.D. acknowledges the International Centre for Genetic Engineering and Biotechnology (UNIDO) for a postdoctoral fellowship.

JA952636+

(43) Bertini, I.; Briganti, F.; Luchinat, C.; Scozzafava, A.; Sola, M. *J. Am. Chem. Soc.* **1991**, *113*, 1237−1245.